

Role of High-Resolution Multidetector Computed Tomography in Characterization of Pulmonary Ground Glass Opacity

Rasha Shawky Zaki*, Osama Abdallah Dawoud, Ayman Fathy Ahmed and Ahmed Fekry Salem

Department of Radiodiagnosis, Faculty of Medicine, Zagazig University, Sharkia, Egypt

*Corresponding author: Rasha Shawky Zaki, Mobile: (+20) 0100 4293609, E-Mail: zakirasha197@yahoo.com

ABSTRACT

Background: Multislice computed tomography not only improves the detection and characterization of parenchymal abnormalities but also increases the accuracy of diagnosis.

Objective: To study and differentiate multidetector computed tomography findings and the pathologic characteristics in different pulmonary ground-glass opacity causes.

Patients and methods: Thirty patients referred from the Chest Department, Zagazig University Hospital to the Radiology Department during the period from November 2018 to December 2019, were included in this cross-sectional trial. Diagnosis of GGO is based on careful history taking and clinical data, restrictive or obstructive pulmonary defect, and conclusive radiographic as well as histopathologic findings.

Results: parenchymal lung diseases were predominant as seen in 24 patients accounting for 80 % of such patients while vascular diseases were responsible for ground-glass attenuation were only 6 patients accounting for 20%. The commonest diagnosis for the diffuse pattern of ground-glass opacity was interstitial lung diseases (16.7%), followed by pulmonary fibrosis (13.3%), cardiogenic pulmonary edema (10%), then pulmonary hemorrhage (6.7%), and lastly pulmonary hypertension with (3.3%). In the patchy pattern of ground glass, the commonest diagnosis was infectious pneumonia (10%), followed by post-irradiation and post patchy and diffuse patterns showing restrictive dysfunction (high FEV1/FVC and FVC is reduced) and the nodular pattern shows mixed dysfunction (low FEV1 and low FVC).

Conclusion: we offer a diagnostic approach for the evaluation of ground-glass patterns in HRCT of the chest based on all previous consensus data. It could help to narrow the list of differential diagnosis and reach the most accurate one.

Keywords: High-Resolution Multidetector Computed Tomography, Ground Glass Opacity.

INTRODUCTION

A hazy opacity on computed tomography scans of the lungs, known as pulmonary ground-glass opacity (GGO), does not conceal the underlying bronchial structures or pulmonary arteries (CT) ⁽¹⁾. On the pathological side, GGO can be produced by partial airspace filling, interstitial thickening with inflammation, edema, and fibrosis, proliferation of malignant cells, the normal state of the respiratory system, or increased pulmonary capillary blood volume. Because of this, CT should be carried out under a set of predetermined guidelines ⁽²⁾.

Depending on the existence of solid components, GGO can be classed as pure (pGGO) or mixed (mGGO). As a non-specific finding on lung CT, GGO may be seen in diseases such as organized pneumonia or localized fibrosis ⁽³⁾. As a result, it has recently garnered a lot of attention because it may suggest early underlying lung cancer, which in most cases appears as a bronchiole-alveolar carcinoma (BAC) and an adenocarcinoma with a BAC component ⁽⁴⁾.

Using a computed tomography (CT) scan, GGO is barely visible or only the solid portion of the lung can be detected in this window. CT scans often show GGOs alongside other interstitial or alveolar abnormalities. As an alveolar finding, GGO denotes partially filled alveoli, and it is frequently found on or near the periphery of the consolidated lung. In some circumstances, active inflammation has been linked to interstitial illnesses. Fine fibrosis can be seen on CT imaging if GGO is found next to interstitial abnormalities ⁽⁵⁾.

Therefore, if all causes of GGOs are grouped,

there is an impossibly broad differential generated, which includes a large number of interstitial diseases and a large array of alveolar diseases ⁽⁵⁾. Because of this, the difference formed by grouping all the causes of GGOs is unreasonably vast, including numerous interstitial disorders and a wide range of alveolar diseases. Detection and diagnosis of lung GGO lesions have improved dramatically with the introduction of HRCT ⁽⁶⁾.

In a single breath-hold, multislice CT can cover a larger area, with better longitudinal and in-plane spatial resolution, as well as superior temporal resolution. Images of the airways, including those generated by techniques developed expressly for airway imaging, such as virtual bronchography and virtual bronchoscopy, can be generated using this data set ⁽⁶⁾.

Workstation-based interpretation of the reconstructed images should be made available or the radiologist at the workstation can undertake interactive picture reconstruction using hard copies ⁽⁷⁾. Many clinical scenarios could benefit from high-quality multiplanar and three-dimensional (3D) pictures ⁽⁸⁾. Multislice computed tomography not only improves the detection and characterization of parenchymal abnormalities but also increases the accuracy of diagnosis ⁽⁹⁾.

To study and differentiate multidetector computed tomography findings and the pathologic characteristics in different pulmonary ground-glass opacity causes was the goal of this study.

PATIENTS AND METHODS

Thirty patients referred from the Chest

Department of Zagazig University Hospital to the Radiology Department during the period from November 2018 to December 2019, were included in this cross-sectional trial. Diagnosis of GGO is based on careful history taking and clinical data, restrictive or obstructive pulmonary defect, and conclusive radiographic and histopathology findings.

Inclusion Criteria: Patients with chest complaints such as cough, chest pain, breathing difficulties, fever, weight loss, hemoptysis, and chest wheeze were referred to the Radiology Department for CT investigation and cases with pulmonary ground-glass opacity were included in the study.

Exclusion Criteria: Pregnant females, patients with deformity in the vertebral column, and patients with previous lung surgery.

Ethical consent:

Approval of the study was obtained from Zagazig University Academic and Ethical Committee (ZU-IRB#6765). Every patient signed informed written consent for the acceptance of participation in the study. This work was carried out following The Code of Ethics of the World Medical Association (Declaration of Helsinki) for studies involving humans.

All studied groups underwent the following

1. History taking: Full history was collected as occupation as well as family history.

2- Clinical examination: General examinations, and vital signs, in addition to a local examination of the chest.

3- Laboratory investigations: Rests were considered according to case e.g. assessment of serum immunoglobulin, sputum analysis

4- Imaging procedures:

A-Chest X-ray: It is firstly performed as it is a relatively cheap test and may help in the diagnosis of the simple condition and it is done in PA view in full inspiration.

B- Multi-detector computed tomography of the chest:

Equipment:

CT scanning was performed for all patients included in this study using Philips core 128 MDCT (Philips ingenuity 128).

Patient position: All patients were scanned in the supine position each patient was instructed to remain stable and did not move during the examination, also breath-holding during scanning time was important and if they were unable to do so, they were instructed to breathe as quietly as possible.

Scanogram: It was done in full inspiration with its superior extent being the superior margin of the clavicle while its inferior extent was the posterior costophrenic

angle.

Scan parameters of MDCT were: (1) Slice thickness: 1.25mm. (2) For each slice, 120 KVp is used, and the current is around 240mA. (3) Tube rotation: 0.6-0.9second (0.75s). (4) Detector collimation: 1mm. (5) Matrix size: 512x512. (6) Small, medium, and large patients had their FOV (field of view) altered. (7) Pitch ~1. (8) Rotation time: 0.5 sec/rotation. (9) Table movement per gantry rotation: 7.5mm. (10) Scan time: 10-20 sec.

Image reconstruction: on our study all examinations were performed on multidetector computed tomography (MDCT) scanners and the acquired images were sent to a PACS system for viewing on the highly specialized workstation. Reconstructed CT image data was evaluated at a window of -450 Hu and 1500 Hu with a high spatial frequency method.

Pulmonary function test: It was done for patients by using forced spirometry. To measure the forced expiratory volume in one second (FEV1), the forced vital capacity (FVC), and the FEV1/FVC ratio, patients were instructed to inhale maximally and then forcibly exhale.

Diagnostic interpretation: Observers looked at the images in turn. Each case was diagnosed and evaluated for category based on the final pathological or clinical diagnosis through radiological correlation and clinical findings in the wake of the diagnostic process.

Statistical analysis

The collected data were coded, processed, and analyzed using the SPSS (Statistical Package for Social Sciences) version 22 for Windows® (IBM SPSS Inc, Chicago, IL, USA). The range (minimum and maximum), mean, standard deviation, median, and interquartile range were used to characterize quantitative data (IQR). To determine the significance of the acquired results, a 5-percent threshold was used. It was a Chi-square test. For categorical variables, chi-square correction for more than 20% of cells with an anticipated count of less than 5 was required, Student t-test: to calculate the quantities of data of normal distribution and to compare between two studied groups. P-value < 0.05 was considered significant.

RESULTS

The mean age of the studied group was (36.8±8.6) ranging between (20 to 54) years, and the age group from (30 to 40 years) was the commonest (50.0%) of the studied group. (53.3%) of the studied group were males and (46.7%) were females. (56.7%) of the studied group were smokers and (43.3%) were non-smokers and cough was the most commonest complaint (60.0%) of the studied cases followed by chest pain (53.3%) & dyspnea (43.3%) then fever (36.7%) and hemoptysis (26.7%) and lastly weight loss (13.3%) and fatigue (6.7%) (**Table 1**).

Table (1): Demographic and complaints distribution among the studied group

| Variable | The studied group No. (30) | |
|--|-------------------------------|-------|
| Age (years): Mean ± SD (Range) Median | 36.8±8.6 (20-54) 37.5 | |
| Age grouping | No. | % |
| <30 years | 5 | 16.7% |
| 30-40 years | 15 | 50.0% |
| 40-50 years | 8 | 26.6% |
| 50-60 years | 2 | 6.7% |
| Sex | | |
| Male | 16 | 53.3% |
| Female | 14 | 46.7% |
| Smoking | | |
| Yes | 17 | 56.7% |
| No | 13 | 43.3% |
| Complaints | | |
| Cough | 18 | 60.0% |
| Chest pain | 16 | 53.3% |
| Dyspnea | 13 | 43.3% |
| fever | 11 | 36.7% |
| Hemoptysis | 2 | 6.7% |
| Weight loss | 4 | 13.3% |
| Fatigue | 2 | 6.7% |

Eighty Percent (80%) of the studied group had parenchymal ground-glass opacity and (20%) had vascular ones (**Table 2**).

Table (2): Causes of ground-glass opacity among the studied group.

| Causes of ground-glass opacity | The studied group | |
|--------------------------------|-------------------|-----|
| | NO(30) | % |
| Parenchymal | 24 | 80% |
| Vascular | 6 | 20% |

Around (36.6%) of the studied group had ground-glass opacity in the right upper lobe, then the right middle lobe (30%), the left upper lobe (26.7%) and the right lower lobe (20%), then the lingual (16.7%) and lastly the left lower lobe (13.3%), **Table (3)**.

Table (3): Percentage of ground-glass opacity location among the studied group

| Ground glass opacity location | NO. (30) | % |
|-------------------------------|----------|-------|
| Right upper lobe | 11 | 36.6% |
| Right middle lobe | 9 | 30% |
| Right lower lobe | 6 | 20% |
| Left upper lobe | 8 | 26.7% |
| Lingual | 5 | 16.7% |
| Left lower lobe | 4 | 13.3% |

Diffuse ground-glass opacity was the most commonest pattern (50%) followed by patchy pattern (26.7%) and nodular type was the least one (23.3%) (**Figure 1**).

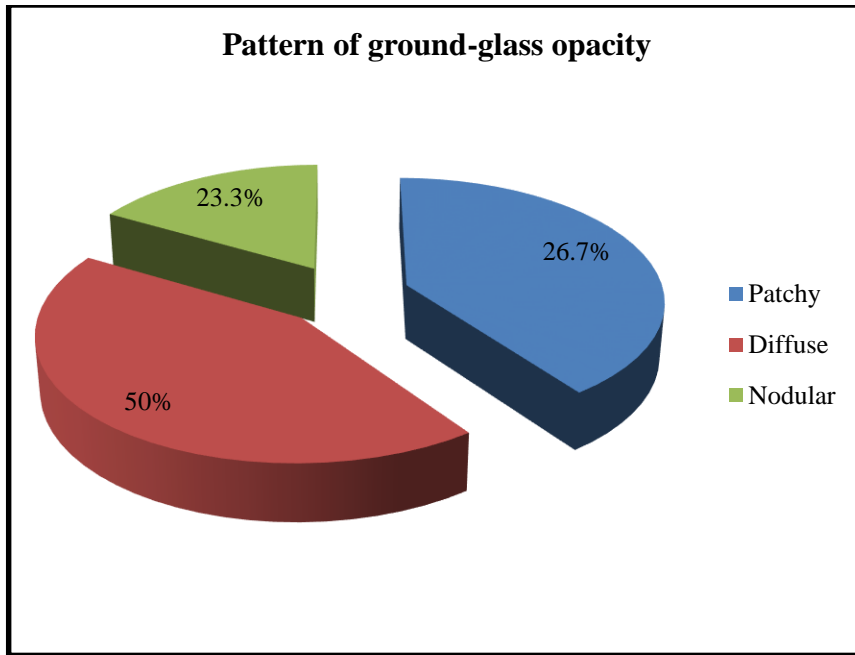


Fig. (1): Pie chart for the pattern of ground-glass opacity in the studied group

There was a statistically significant increase in FVC % in non-smokers than smokers. But regarding FEV1 % and FEV1 / FVC %, there was no statistically significant difference between non-smokers and smokers (**Table 4**).

Table (4): Comparing pulmonary function tests between smokers and non-smokers

| Variables | Smokers (17) mean ± SD | Non-smokers (13) mean ± SD | t-test | p-value |
|---------------------|---------------------------|-------------------------------|--------|---------------|
| <i>FEV1 %</i> | 70.4±17.3 | 82.1±6.6 | 1.8 | 0.09 |
| <i>FVC %</i> | 66.4±7.2 | 79.4±10.3 | 3.4 | 0.003* |
| <i>FEV1 / FVC %</i> | 1.04±0.2 | 1.07±0.15 | 0.3 | 0.7 |

There was a statistically significant difference, according to the pattern of GGO and pulmonary function tests, as patchy and diffuse patterns showing restrictive dysfunction (high FEV1/FVC and FVC is reduced) and nodular patterns show mixed dysfunction (low FEV1 and low FVC) (**Table 5**).

Table (5): Comparing pulmonary function tests between patients with different patterns of ground-glass opacity.

| Variables | Patchy (8) mean ± SD range | Diffuse (15) mean ± SD range | Nodular (7) mean ± SD range | t-test | p-value |
|---------------------|----------------------------------|------------------------------------|-----------------------------------|--------|---------------|
| <i>FEV1 %</i> | 80.2±7.9 (70-90) | 77.6±7.5 (68-88) | 56.1±12.8 (35-88) | 6.4 | 0.007* |
| <i>FVC %</i> | 70.5±5.2 (62-77) | 75.2±14.3 (55-96) | 63.8±9.4 (54-76) | 1.9 | 0.2 |
| <i>FEV1 / FVC %</i> | 1.13±0.04 (1.04-1.18) | 1.06±0.19 (0.77-1.31) | 0.8±0.2 (0.64-1.16) | 5.6 | 0.01* |

Interstitial lung diseases were the commonest diagnosis for the diffuse pattern of ground-glass patients (16.7%), followed by pulmonary fibrosis (13.3%), then cardiogenic pulmonary edema with (10%), and infectious pneumonia was the commonest diagnosis for the patchy pattern of ground-glass patients (10%), followed by post-irradiation and post-chemotherapy pneumonitis with (6.7%) for each one, hypersensitivity pneumonitis was the commonest diagnosis for the nodular pattern of ground-glass patients (10%), followed by tuberculosis and metastatic pulmonary nodules with (6.7%) for each one (**Table 6**).

Table (6): Distribution of patients with diffuse, nodular, and patchy ground-glass attenuations.

| Diffuse ground glass | Number of patients | % of total Diffuse pattern | % of total GG |
|-------------------------------|--------------------|----------------------------|---------------|
| Interstitial lung diseases | 5 | 33.3 | 16.7 |
| Cardiogenic pulmonary edema | 3 | 20 | 10 |
| Pulmonary hemorrhage | 2 | 13.3 | 6.7 |
| Pulmonary fibrosis | 4 | 26.7 | 13.3 |
| Pulmonary hypertension | 1 | 6.7 | 3.3 |
| Total | 15 | 100 | 50 |
| Patchy ground glass | Number of patients | % of total Patchy pattern | % of total GG |
| Post irradiation pneumonitis | 2 | 25 | 6.7 |
| Post chemotherapy pneumonitis | 2 | 25 | 6.7 |
| Infectious pneumonia | 3 | 37.5 | 10 |
| Bronchoalveolar carcinoma | 1 | 12.5 | 3.3 |
| Total | 8 | 100 | 26.7 |
| Nodular ground glass | Number of patients | % of total nodular pattern | % of total GG |
| Hypersensitivity pneumonitis | 3 | 42.8 | 10 |
| tuberculosis | 2 | 28.6 | 6.7 |
| Metastatic pulmonary nodules | 2 | 28.6 | 6.7 |
| Total | 7 | 100 | 23.3 |

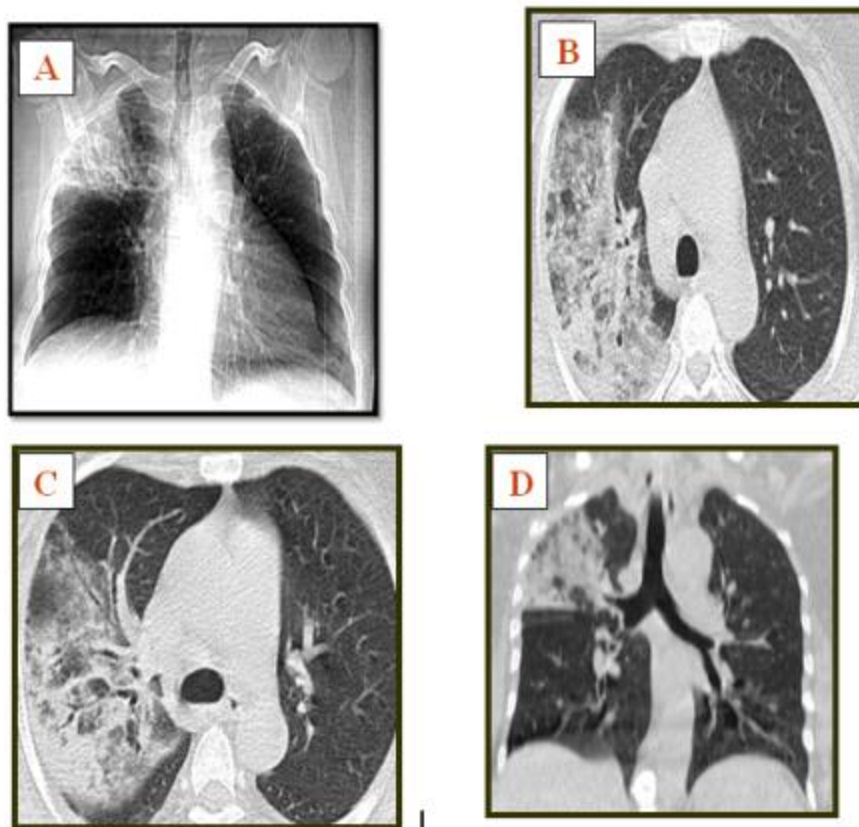


Fig. (2): Female patient 39 years old with complaints of fever, cough, and dyspnea. (A) plain X. ray (B & C) CT lung window axial view (D) CT lung window coronal view (E) CT mediastinal window axial view (F) CT mediastinal window coronal view showing: right lung upper lobe segmental areas of ground-glass opacities with bilateral coarse pulmonary reticulations and large wedge-shaped consolidated area seen at the upper lobe of the right lung with air bronchogram inside it the appearance refer to lobar pneumonia.

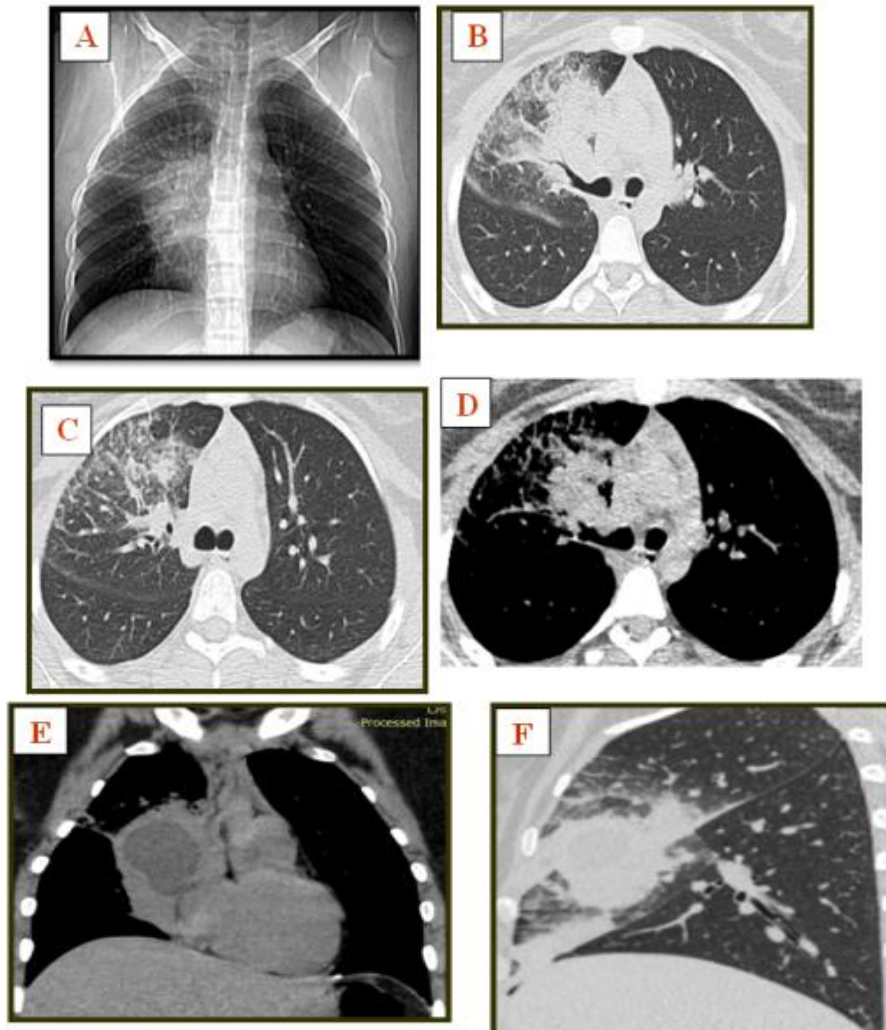


Fig. (3): Female patient 25 years old, known pericardial abscess with complaints of fever, chest pain, fatigue, and dyspnea. (A) Plain X. ray (B & C) CT lung window axial view (D) CT mediastinal window axial view (E) CT mediastinal window coronal view (F) CT lung window sagittal view showing: pericardial abscess right upper lobe area of ground-glass opacity with reticular infiltration representing interstitial pneumonia.

DISCUSSION

Differential diagnoses can be narrowed down by utilizing a systematic approach to classify GGO based on its form, distribution, and any accompanying imaging findings, such as the presence of cysts or traction bronchiectasis, or air trapping. A patient's history of symptoms, such as how long they've lasted or how well their immune system is functioning, is critical. Imaging patterns and pertinent clinical information can help radiologists make an accurate and concise differential diagnosis for GGO, which is a nonspecific finding⁽¹⁰⁾.

In the current study, diagnosis of GGO was based on careful history taking and clinical data, restrictive or obstructive pulmonary defect, and conclusive radiographic or histopathology findings. Pregnant females and those with extensive spinal deformities were excluded from this study.

An investigation was conducted to examine the role of multi-detector CT in assessing pulmonary ground-glass opacity. Our ability to generate extremely spatially precise volumetric pictures of the lung during a single breath-hold was greatly enhanced by the development of multi-detector row CT (MDCT). A near

isotropic voxel volumetric image of the lung may now be obtained with breath holds of less than 5 seconds thanks to the rapid development of 128-slice scanners and beyond. Using these images, a radiologist can subjectively detect and quantify the presence and degree of disease, whereas a computer uses these images to objectively detect and quantify the existence of disease⁽¹¹⁾. In our study 30 patients with GGO were included 16 male (53.3%) and 14 female (46.7%) with an average age was 36.8 ± 8.6 years, ranging from 20 to 54 years old which is nearly inconsistent with **Shah et al.**⁽¹²⁾ reported that GGO was 56.7% in males and 43.3% in females, with a mean age of 51.4 years.

Smoking history in this study was 56.7% of cases and non-smokers were 43.3% which was similar to the study reported by **Chang et al.**⁽¹³⁾ stated that smokers with GGO were representing 66% of cases and non-smokers were 34%.

The common site of pulmonary ground-glass opacity in our study was the right upper lobe 36.6%, then the right middle lobe 30%, followed by the left upper lobe 26.7%, then the right lower lobe 20%, then lingual 16.7%, and lastly left lower lobe 13.3%. **Yu, et al.**⁽¹⁴⁾ reported that the location of GGO in the right

upper lobe was 26%, the right middle lobe was 19.8%, the left upper lobe was 17.9%, the right lower lobe 14.2%, the lingula 14.2%, and the left lower lobe 7.5%.

Concerning the clinical picture, the most common complaint was cough presented in 18 patients (60%), 16 patients with chest pain (53.3%), 13 patients with dyspnea (43.3%), 11 patients with fever (36.7%), 8 patients with hemoptysis (26.7%), 4 patients with weight loss (13.3%) and 2 patients with fatigue (6.7%). That was nearly in agreement with **Yu et al.** (14) who stated that the most common symptoms in GGO were chest pain (59.4%) followed by cough (53.7%) then dyspnea (33.9%) then hemoptysis (26.4%). Regarding the ground glass opacity in our study it was categorized into three main patterns:

Diffuse pattern of distribution was the most common pattern seen in 15 patients accounting for around 50%, patchy or lobular pattern was next seen in 8 patients accounting for around 26.7% lastly, and the nodular pattern was seen in 7 patients accounting for around 23.3%. Regarding **Shah et al.** (12) Ground-glass opacity was most commonly diffusely distributed (43%), followed by lobular (41%) and nodular (16%).

In our study, patients with diffuse GGO were presented with cardiogenic pulmonary edema associated with cardiac chamber enlargement which was seen in 10% of cases. Pulmonary hemorrhage due to trauma was 6.7% and pulmonary hypertension was 3.3%, which is nearly inconsistent with a study carried out by **Miller et al.** (10) who stated that the causes of diffuse ground-glass opacity, DAH, cardiogenic edema, and non-cardiogenic pulmonary edema accounted for 19 percent of all acute alveolar disorders.

Chronic interstitial lung diseases with diffuse ground-glass attenuation and reticular lung patterns were found in 16.7% of cases. And diffuse pulmonary fibrosis complicated by honey combing and bronchiectasis were seen in 13.3% of cases. Regarding **Miller et al.** (10) 27 percent of the causes of diffuse GGO in chronic diffuse interstitial lung disorders.

In this study, patchy or lobular ground-glass attenuation, and viral or bacterial pneumonitis were found in 10% of patients with a history of fever and toxemia, and CT findings in the form of septal thickening and consolidation. In comparison to a study by **Miller et al.** (10), ground-glass opacity was most frequently associated with acute atypical pneumonia and diffuse infections particularly *Pneumocystis carinii* pneumonia (PCP) are among the most common causes accounted 32%.

Drug-induced pneumonitis, in our study, was found in 13.3% of cases with a positive history of irradiation and chemotherapy including patchy areas of ground-glass attenuation with mild reticular thickening, air trapping, or consolidation, which is nearly inconsistent with a study carried out by **Miller et al.** (10) stated that drug toxicity represented 11% of cases in Chemotherapy patient with cancer that has spread to the bone marrow. Because of their neutropenia and

thrombocytopenia, these individuals were at risk for opportunistic infections.

Broncho-alveolar carcinoma presented in 3.3% of cases with consolidation, ground-glass opacities, and air-space nodules, which is similar to a study carried out by **Akira et al.** (15) who reported that broncho-alveolar carcinoma appears as ground-glass opacity represented by 10.5% of cases.

Nodular ground-glass opacity in this study presented in hypersensitivity pneumonitis with a history of exposure to a certain allergen (most commonly seen with raising birds) lacking smoking history and presented in 10% of cases. **More et al.** (16) reported that in hypersensitivity pneumonitis due to Bird fanciers, the common chest CT features were ground-glass areas in (68%) of cases.

Metastatic pulmonary nodules presented in 6.7% of cases, with ground-glass opacity, with a history of primary cancer, which is nearly inconsistent with **Beom et al.** (17) said that nodular attenuation surrounded by ground-glass opacity on CT is a very typical observation in lung metastasis with accompanying tumor bleeding.

Obstructive or restrictive breathing problems can be detected using spirometry and the FEV1/FVC formula, according to pulmonary function testing. Having an FEV1/FVC ratio of less than 70 percent indicates an obstructive problem. The predictive value of the FEV1 can be expressed as a percentage, allowing the degree of impairment to be determined. Restrictive abnormalities, such as interstitial lung disorders, can cause an FEV1/FVC ratio greater than 70%, which indicates a reduction in FVC (e.g. idiopathic pulmonary fibrosis) (18).

There were statistically significant differences in FVC %, FEV1%, and FEV1/FVC % values between non-smokers and smokers, as all pulmonary function values decreased in smokers in comparison to non-smokers. This was similar to a study carried out by **Lubinski et al.** (19) and **Aydin et al.** (20) who stated that there was a reduction of different values of PFTs among smokers compared with non-smokers.

According to the pattern of ground-glass opacity between smokers and non-smokers, there was a statistically significant difference, as all nodular patients were smokers. But patients with diffuse patterns most of them were non-smokers. This was similar to a study carried out by **Chang et al.** (13) who stated that most of the nodular ground-glass were smokers.

There was a statistically significant difference between pulmonary function tests and pattern of ground-glass opacity where patchy and diffuse patterns showed restrictive dysfunction (high FEV1/FVC and FVC is reduced) while nodular patterns showed mixed dysfunction (low FEV1 and low FVC).

These results were in agreement with the results of **Hussein et al.** (21) who reported that FEV1 % and FEV1 / FVC % decrease in nodular ground-glass

pattern, as the nodular pattern is associated with mixed dysfunction. This is attributed to the affection of interlobular and intralobular septal interstitium resulting in airway obstruction. While patchy and diffuse patterns exhibited restrictive dysfunction and this is due to the affection of alveoli and interstitial compartments not related to small airways.

CONCLUSION

MDCT and multi-planar reconstruction provide more data and better characterize ground-glass attenuation than plain chest radiographs. D.D of diffuse G.G is based upon; distribution, associated findings such as septal thickening and mild traction bronchiectasis, cystic bronchiectasis and mucous plugging, honey combing, presence of lung cysts or background of emphysema

Patchy lobular ground-glass opacities are divided into two major categories. The first is associated with fever and toxemia, the other not. The first category includes bacterial and viral pneumonitis. The second category includes drug-induced or post-irradiation pneumonitis, BAC. Differentiation is based upon mixed data about; History and clinical examination, as well as GG distribution, and associated HRCT findings. Multiple GG nodules are seen in TB, HP, and metastasis nodules which are best differentiated using clinical history, also radiological distribution, and other HRCT findings.

Finally, we offer a diagnostic approach for the evaluation of ground-glass patterns in HRCT of the chest based on all previous consensus data. It could help in narrowing the list of differential diagnosis and reaching the most accurate one. Our goal is to reduce the need for lung biopsy and save patients from its hazards.

Conflict of interest: The authors declare no conflict of interest.

Sources of funding: This research did not receive any specific grant from funding agencies in the public, commercial, or not-for-profit sectors.

Author contribution: Authors contributed equally to the study.

REFERENCES

1. **Austin J, Müller N, Friedman P (1996):** Glossary of terms for CT of the lung: recommendations of the Nomenclature Committee of the Fleischner Society. *Radiology*, 200: 327–31.
2. **Kalra M, Maher M, Rizzo S et al. (2004):** Radiation exposure from chest CT: issues and strategies. *J Korean Med Sci.*, 19:159-66.
3. **Nakajima R, Yokose T, Kakinuma R (2002):** Localized pure ground-glass opacity on high-resolution CT: histologic characteristics. *J Comput Assist Tomogr.*, 26:323–9.
4. **Kim H, Shim Y, Lee K et al. (2007):** Persistent pulmonary nodular ground-glass opacity at thin-section CT: histopathologic comparisons. *Radiology*, 245:267-75.
5. **Song Y, Zhan P (2009):** Management and differential diagnosis of ground-glass opacity pulmonary lesions. *Zhonghua Jie He He Hu Xi Za Zhi.*, 32:808–809.
6. **Grenier P, Beigelman-Aubry C, Fetita C et al. (2002):** New frontiers in CT imaging of airways disease. *Eur Radiol.*, 12:1022–44.
7. **Prokop M, Galanski M (2003):** Spiral and multislice computed tomography of the body. Thieme Publishing Group. ISBN: Hardback. Pp. 252-276. <https://www.thieme.com/books-main/radiology/product/2592-spiral-and-multislice-computed-tomography-of-the-body>
8. **Rubin G (2003):** 3-D imaging with MDCT. *Eur J Radiol.*, 45(1): 37–41.
9. **Reiser M, Becker C, Nikolaou K et al. (2009):** Multislice CT. 3rd Revised Edition. Springer-Verlag Berlin Heidelberg, Pp. 193-321. <https://rlmc.edu.pk/themes/images/gallery/library/books/Radiology/A.%20L.%20Baert,%20Maximilian%20F.%20Reiser,%20C.R.%20Becker,%20Konstantin%20Nikolaou,%20Gary%20Glazer%20Multislice%20CT%203rd%20Edition%20Medical%20Radiology%20Diagnostic%20Imaging%202008.pdf>
10. **Miller W, Shah R (2005):** Isolated Diffuse Ground-glass Opacity in Thoracic CT: Causes and clinical presentations. *AJR.*, 184: 613–622.
11. **Rogliani P, Mura M (2008):** HRCT and histopathological evaluation of fibrosis and tissue destruction in IPF associated with pulmonary emphysema. *Respiratory Medicine*, 102: 1753-1761.
12. **Shah R, Miller W (2003):** Widespread ground-glass opacity in consecutive cases: does lobular distribution assist diagnosis? *AJR.*, 180:965–968.
13. **Chang B, Hwang J, Choi Y et al. (2013):** Natural history of pure ground-glass opacity nodules detected by low dose CT scan. *Chest*, 143:172-8.
14. **Yu H, Liu S, Zhang C et al. (2018):** Computed tomography and pathology evaluation of lung ground-glass opacity. *Exp Ther Med.*, 16(6): 5305–5309.
15. **Akira M, Atagi S, Kawahara M et al. (1999):** High-resolution CT Findings of Diffuse Bronchioloalveolar Carcinoma in 38 Patients. *AJR Am J Roentgenol.*, 173(6):1623-9.
16. **Morell F, Roger A, Reyes L et al. (2008):** Bird Fancier's Lung: A Series of 86 Patients. *Medicine (Baltimore)*, 87(2):110-30.
17. **Beom J, Im J, Goo J et al. (2001):** Atypical pulmonary metastases: Spectrum of radiologic findings. *Radiographics*, 21(2):403-17.
18. **He H, Stein M, Zalta B et al. (2006):** Pulmonary infarction: spectrum of findings on multidetector helical CT. *J Thorac Imaging*, 21 (1): 1-7.
19. **Lubinski W, Argowski T, Frank-piskorska A (2000):** evaluation of tobacco smoking on pulmonary function in young men. *Pneumonol Alergol Pol.*, 68: 226-231.
20. **Aydin O, Dursan A, Kurt B et al. (2008):** correlation of functional and radiological finding in asymptomatic smokers. *Turkish Respir J.*, 9: 15-19.
21. **Hussein K, Shaaban L, Mohamed E (2016):** Correlation of high-resolution CT patterns with pulmonary function tests in patients with interstitial lung diseases. *Egyptian Journal of Chest Diseases and Tuberculosis*, 65(3): 681-688.